

High Resolution Bathymetric and Satellite mapping of Gubi Dam Bauchi State, Nigeria

^aShuaibu, M. A., ^bMuhammed, I., ^aMusa, S. I. and ^cMuhammed, I.

^aDept of Surveying and Geoinformatics, Abubakar Tafawa Balewa University Bauchi, Nigeria

^bDept of Surveying and Geoinformatics, Modibbo Adama University of Technology, Yola, Nigeria

^cDept of Hydrography, Office of the Surveyor General of the Federation, Abuja, Nigeria

*Correspondence email: mashuaibu@atbu.edu.ng

Abstract

There is a global concern about the rate of depletion of water reservoirs due to increase in demand and stagnation of supply amid population increase and climate change. Therefore, understanding and managing dams through strategic planning and sustainable-related policies is necessary. The objective of this paper is to examine the current condition of Gubi Dam and change pattern in relation to causes of the change. The dam was sampled using acoustic side-scan sonar and mapped the bathymetry to compute volume and capacity using Trapezoidal, Simpson's Rule and Simpson's 3/8 Rule. Results show astonishing similarity between the three methods, although overestimation in volume with over $1 \times 10^5 \text{ m}^3$ was observed with Simpson's Rule. Landsat 8 OLI/TIRS was used to corroborate these findings. Water surface area shows continuous decline from 2014-2020. The surface area shows similarity to the overall terrestrial surface temperature computed, indicating some level of evaporation. However, recent change in government policy in agricultural has pushed most inhabitants around Gubi Dam and its recharging rivers and streams back to farming. Irrigated farming during the dry season, hence increased usage of Gubi Dam and affected recharge from the rivers. Rural-urban migration to Bauchi metropolis could also increase water usage because the city depends solely on the dam. Annual bathymetric mapping, provision of gauge rainfall data and fixing of water level measurements at both the dam and the recharging rivers and streams are suggested. Sustainability measures relating to core environmental values, issues and threats be examined to guide research and policy thrust.

Keywords: Acoustic, Side Scan Sonar, Bathymetry, Landsat 8, Water Surface, Volume

INTRODUCTION

Land surface water bodies, such as rivers, dams, lakes and reservoirs whether natural or man-made are important to the global water cycle and the global ecosystem in general. Surveying land surface water bodies and delineating their spatial distribution are significant to the understanding of hydrology processes for the purposes of planning, developing and managing water resources (Roberts *et al.*, 1993; Vorosmarty *et al.*; 1997; Papa *et al.*, 2008). Spatial distribution of land surface water reflects the storage and usage status of water resources on land surface (Foley *et al.*, 2005), while its fluctuation or change implies influence on water movement, chemical matter migration and ecosystem sustainability by climatic change (Oki and Kanae, 2006).

The availability of water in sufficient quantities for supply to persons in cities of developing countries is still problematic (Connor, 2015). At present and for the foreseeable future, due to population growth, economic development, and accelerated urbanisation, coupled with the

intensifying impact of climate change, water security problems will become increasingly prominent, posing a major challenge to sustainable development (World Water Council, 2018).

In terms of water and sanitation, more than 1.1 billion people lack access to safe drinking water and 2.6 billion people do not have access to sanitation facilities as at 2018, and 650,000 children die of water-borne diseases every year. In terms of water and food, it is expected that by 2050 global grain output will need to increase by 60% and agricultural water use by 55% to meet the food demand of the growing world population (World Water Council, 2018).

Many sanitary issues relating to health disorders in urban areas of developing countries have been traced to lack of adequate water supply (Khatri and Tyagi, 2015). Apart from drinking, water is needed to meet the challenging requirements of sewage, medical, industrial and other applications (Larsen *et al.*, 2016). Sources of water (pond, rivers, streams, dams etc) are either far located or found closely constructed but inadequate for sustainable supply to urban areas. In 2019 water supply forecast, more than 1.8 million people will be lacking water in developing countries (Boretti and Rosa, 2019).

The use of dam to store water for water treatment and supply to urban areas is still cost-effective and more efficient as compared to creation of boreholes and changing streams (Page *et al.*, 2018). Dam is created based on designed capacity to cater for the identified and intended needs of an area. Population growth, irrigation activities and other industrial applications had put much pressure on the dams (Bhattacharjee and Nayak, 2019; Enqvist and Ziervogel, 2019).

Damming also has implications of flow control of river catchments. The geometric variables are reduction in the overall channel width, concave bank erosion and emergence of vegetation in some of the reaches (Tukur and Mubi, 2002). All these can be monitored using bathymetric and remote sensing sampling techniques.

Several previous studies (e.g. Parnum *et al.*, 2009; Schimel *et al.*, 2010; Serpetti *et al.*, 2011; Haris *et al.*, 2012) have studied and compared the performances of single-beam and multibeam echo sounder data for bathymetric mapping, often through the use of automated or semi-automated methods for acoustic ground discrimination and habitat interpretation, with an emphasis on physical habitats. These studies showed advantages of these technologies where by multibeam is much required for large-scale mapping purposes. In a smaller river or continental reservoirs, the single beam suffices.

Schimel *et al.* (2010b) identified the relative merits of side scan sonar compared to other seabed mapping technologies for underwater mapping and found that in the absence of the need to discriminate sediment type or provide a proxy to benthic habitat, side scan sonar is good enough. A feasibility study by Elvenes *et al.* (2012) shows that the potential use of alternative full-coverage data sources for regional sediment mapping that include side scan sonar is recommended for small scale mapping while multibeam in addition to other instruments are required for full sediment budget.

The role of water to agriculture is critical for understanding issues affecting productivity and sustained livelihoods of local farmers. Improved productivity leads to a sustained human wellbeing through economic development. Monitoring water bodies and its resultant consequences are basic applications in satellite remote sensing. Pragmatic and logical reasons in the use of remote sensing lies in its ability to capture a wide area, a lot of times using index-based analysis. Remote sensing has become a routine approach for land surface water body monitoring, because the acquired data can provide near real time and cost effective information which is substantially different from conventional survey methods. Measuring and monitoring

surface water using remote sensing is therefore an essential topic in many research areas, including flood-related studies and water resource management (Foley *et al.*, 2005).

Index based remote sensing analysis require understanding and processing certain wavelengths of surface reflectance to arrive at results. The wavelengths are dependent on satellite sensor type and designation to which the geophysical quantities are determined. The nomenclature of bands with varying wavelengths in one satellite differ from another satellite irrespective of their footprint, the instantaneous field of view (IFOV) or the resolution of spatial data. For example, band designation for any Landsat is different from that of MODIS (Moderate Resolution Imaging Spectroradiometer) or Sentinel. For example, Landsat 8 (infrared – band 5) has a wavelength of 0.845–0.885 while Sentinel 2 (infrared – band 5) is 0.785 - 0.900. With this, even if they could be of the same spatial resolution taken same time will have difference in results because the spectral signature measured by each satellite is different from the other. Advances in satellite remote sensing particularly on spatial, spectral and temporal resolution provide an abundant data that become primary sources for detecting and extracting water surface and its changes (Xu, 2006; Zhou *et al.*, 2011). Landsat data is widely used for water body detection and extraction as well as change detection over time (Tang *et al.*, 2013; Li *et al.*, 2013).

Normalised Difference Water Index (NDWI) (Gao, 1996) has been used to quantify vegetation liquid water status from space, the reflectance properties of green vegetation, dry vegetation and soils after atmospheric correction using two infrared channels. It is further considered as an appropriate water absorption index for comparison with NDVI (Sims and Gamon, 2003). Near infrared and green bands were used by McFeeters (1996) to delineate open water features based on the fact that infrared has high absorption rate of water while red does not. Because the NDWI was found to be sensitive to background soil, it is good in estimated shallow water bodies to allow a clear delineation of water boundaries. Land surface temperature (LST) is one of the key parameters in land–surface physical processes on regional and global scales and has been widely applied to hydrology, meteorology and the surface energy balance (Wan and Dozier, 1996; Valor and Caselles, 1996 and Cheng *et al.*, 2010). It gives the background and instantaneous changes over space and time of temperature and other related geophysical information of land surface such as evapotranspiration. Remote sensing provides this unique way of obtaining the LST at local, regional and global scales. Various LST products from different satellites have been widely used in the urban ecological environment, water management and natural disasters (Weng *et al.*, 2004; Manzo-Delgado *et al.*, 2009).

Bauchi metropolis depend solely on Gubi Dam for its water usage. However, siltation and sedimentation have reduced the capacity of the dam over the years, hence the necessity to monitor it (Loucks and VanBeek, 2017). Therefore, this study focuses on bathymetric mapping, modeling the depths, delineating its surface area and examining the temperature condition of the lake and its surrounding area to examine its dynamics and causes of change. This is to obtain in addition to the physical conditions, the dam capacity and volume as well as changes over time. This study employs single beam echo sounder as well as satellite remote sensing water indices to evaluate the capability of linking multiplatform and multisensor instruments for mapping a reservoir.

Study area

The study area is Gubi Dam, located in Firo, Ganjuwa Local Government Area of Bauchi State centred at (longitude 10° 25' 5.88", latitude 9° 52' 51.9594"). The Dam lies to the northeast of

the Bauchi metropolis, about six kilometers away from it. The source of water in Gubi Dam are three tributaries, namely Gubi River, Tagwaye river link with Shadawanka and Ran River. Tatimari (Shadawanka and Dinya), Suntum, Kumi and Larkarina provide the major tributaries to the dam (Wufem *et al*, 2009). The dam was constructed in 1979 to serve as a permanent water supply scheme for irrigation and dairy farming to Bauchi and its environs. The function of the dam is to supply the state capital and its environs with potable water. A temporary dam close to the site was constructed across one of the streams to provide water needed for the construction of the permanent dam as well as for municipal usage. This small impounded dam produced over 500 million gallons (1, 892, 706m³) prior to the completion of Gubi Dam. Gubi Dam’s embankment has a length of 3.86km and bottom earth-fill of 2,315, 000m³ with a reservoir area of 590 hectares. The catchments area is 17, 900 hectares with total storage capacity of 38.4 x 10⁶ m³, the expected yield from the reservoir is 90,000m³/d (Bauchi State Water Board, 1981). The region is classified as tropical, and the annual rainfall in the dam basin ranges from 970mm to 1400mm with about 50 to 60% of this rainfall occurring between July and August. Fishing, recreation, irrigation, dairy farming and water treatment take place around the dam (BASWAB, 1990).

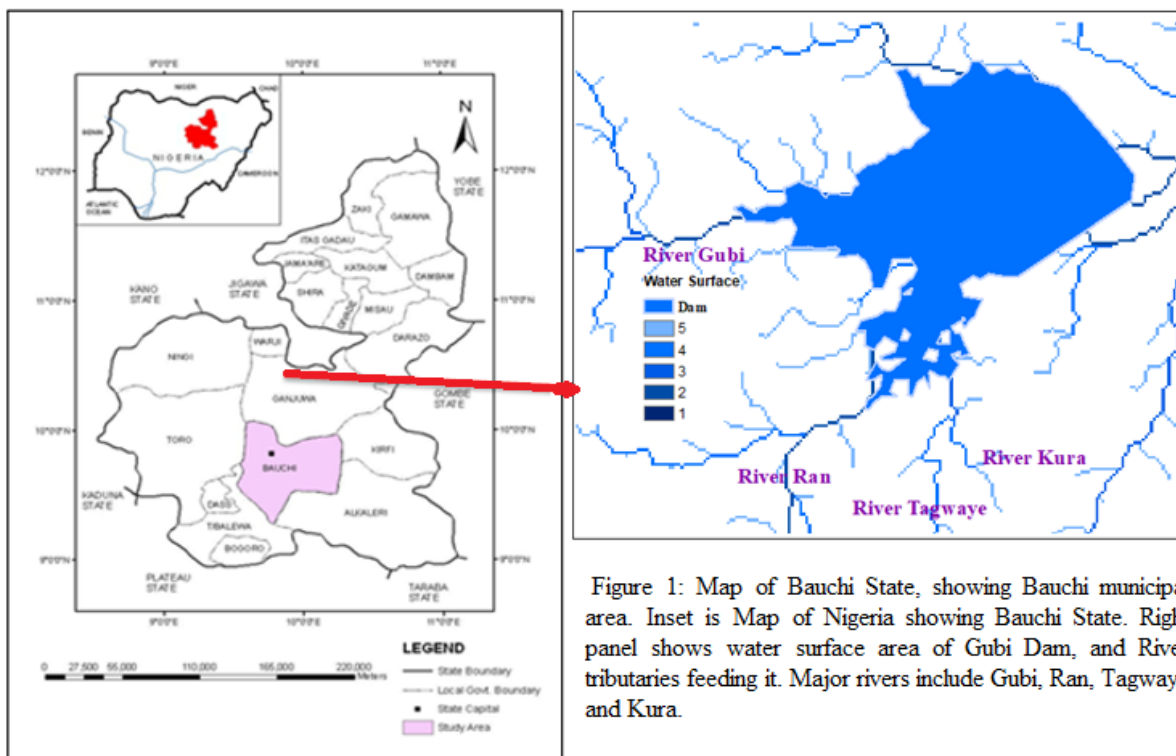


Figure 1: Map of Bauchi State, showing Bauchi municipal area. Inset is Map of Nigeria showing Bauchi State. Right panel shows water surface area of Gubi Dam, and River tributaries feeding it. Major rivers include Gubi, Ran, Tagwaye and Kura.

MATERIALS AND METHODS

Materials

The datasets used in this study are bathymetry sampling and optical data from Landsat 8 Operational Land Imager (OLI) and Thermal Infrared Sensor (TIRS) bands. The bands employed for LST were 3, 4, 5 and 10 (table 1). These data were chosen for March of each year to get a minimal cloud contamination of less than 2%. The years were 2014, 2015, 2017, 2019 and 2020. The years 2016 and 2018 were not sampled because the thermal bands for March of these years and even close by months such as January, February, April and May could not give good results due to cloud contamination on the TIRS band.

Table 1: Landsat 8 OLI/TIRS for March of various years with cloud cover less than 2%. The path/row of 187/53. The datum is UTM (zone 32) and the projection is WGS84.

Band	Name	Wavelength (μm)	Spatial resolution (m)
2	Blue	0.45-0.51	30
3	Green	0.53-0.59	30
4	Red	0.64-0.67	30
5	NIR	0.85-0.88	30
6	SWIR1	1.57-1.65	30
10	TIRS	10.6-11.19	100 (re-gridded to 30)

Methods

Echo Sounding

The first data required for this study was obtained using bathymetric survey in July 2019 through the use of high resolution Digital Single Beam Echo Sounder equipment and its accessories. The grid at 25m interval with overlap method of data acquisition was adopted for the xyz data in order to determine the depth. At the end of the track lines a close loop survey of the dam was measured. The loop allowed the coverage of the entire perimeter of the dam and for the determination of the total area.

Volume Determination

Due to the irregular nature of the dam, certain factors such as the shape of the water body, size, units and the software were considered. Hence, Trapezium Rule was used because in this method, the entire dam was divided into plan view sections and the cross-sectional areas were determined from depths relative to chart datum. Then, the plan distance between each cross-section was used to obtain the dam volume. The 3D terrain model of the chart plotted in surfer was then used to calculate the volume of water in the dam. Trapezoidal Rule, Simpson’s Rule and Simpson’s 3/8 Rule algorithms were also applied in computing the volume of the water and all tend to give similar results.

The *trapezoidal rule* is a technique for approximating the definite integral of the area under a curve is evaluated by dividing the total area into little trapezoids rather than rectangles.

$$\int_a^b f(x) dx.$$

Simpson's Rule is a numerical method that approximates the value of a definite integral by using quadratic functions. It’s a method employed where all other methods are not possible. Specifically, it is the following approximation for $n + 1$ values x_0, \dots, x_n , bounding n equally spaced subdivisions (where n is even):

$$\int_a^b f(x) dx \approx \frac{\Delta x}{3} (f(x_0) + 4f(x_1) + 2f(x_2) + 4f(x_3) + 2f(x_4) + \dots + 4f(x_{n-1}) + f(x_n)).$$

where $\Delta x = \frac{b - a}{n}$ and $x_i = a + i\Delta x$.

Simpson's 3/8 Rule is another method for numerical integration. Just the Simpson's rule described above, but this is based upon a cubic interpolation rather than a quadratic interpolation. Simpson's 3/8 rule is as follows:

$$\int_a^b f(x) dx \approx \frac{3h}{8} \left[f(a) + 3f\left(\frac{2a+b}{3}\right) + 3f\left(\frac{a+2b}{3}\right) + f(b) \right] = \frac{(b-a)}{8} \left[f(a) + 3f\left(\frac{2a+b}{3}\right) + 3f\left(\frac{a+2b}{3}\right) + f(b) \right],$$

where, $b-a=3h$

Dam capacity

The dam capacity is the water carrying capacity and is computed via the formula:

$Dc = (\text{width} * \text{Depth} * \text{length}) \text{ ft}^3$ (in gallons) to be converted to m^3 .

Delineating water surface area

Water surface area of the dam was delineated based on McFeeters (1996) normalised difference water index (NDWI) using Landsat 8 data. This index shows the boundaries of water and non-water surfaces only. The result in raster is now converted to vector to allow surface water coverage be calculated. The bands considered and the formula are shown in table 1 and the equation as follows:

$$\text{NDWI} = [\text{Green (Band3)} - \text{NIR (Band5)}] / [\text{Green (Band3)} + \text{NIR (Band5)}]$$

Calculating land surface temperature

The procedure adopted in computing Land Surface Temperature (LST) are based on Ghaleb *et al* (2015) and Azua (2020). Table 2 shows variables required in the computation of LST from the raw DN data using additional information given in the metadata file to finally obtain LST in degree Celsius. The band specific thermal conversion constants, spectral radiance at sensor aperture, centre wavelength of band 10 as well as other constants are used to obtain brightness temperature (BT). Band 10 was chosen because Band 11 which is also a thermal band has inconsistencies. The normalised difference vegetation index (NDVI) was used to compute proportion of vegetation (PV) and in combination with land surface emissivity (ϵ) to give LST in Kelvin, then converted to Celsius. All the formulae are shown in table 2.

RESULTS AND DISCUSSION

The results obtained during the survey represent the current condition of Gubi Dam reservoir (table 3). A net capacity of $87,847,976.34 \text{ m}^3$ of water was revealed in the dam reservoir (table 3). The total volume of water obtained in the dam could be related to the months of August, September and October when the dam reservoir is at its peak due to the raining season. The capacity computed if compared with total volume indicate little difference, indicating that the dam was almost full at the time of sonar sampling end of July 2019. Three survey techniques for computing volume were also determined, and the results gave a striking similarity, especially Trapezoidal and Simpson's 3/8 Rules. The Simpson's Rule technique alone appear to overestimate the volume with over $1 \times 10^5 \text{ m}^3$, likely because its use of quadratic function. The other two rules can be compared with the capacity of the dam.

The digital terrain model (DTM) of the dam reservoir displayed the current depth as at July 2019 (figure 2). This DTM was useful in computing the total volume of the water in the reservoir as well as the dam capacity (table 3). The dam covers a large area with minimum

Table 2: Parameters and steps in computing Land Surface Temperature

Processing step	Formula	Steps	Value	Unit
Conversion of DN to at-satellite brightness temperature	$TB = K2 / \ln((K1/L\lambda) + 1)$	Band-specific thermal conversion constants	$K1 = 774.8853$ $K2 = 1321.0789$	watts/meter squared * ster * μm ;
		Spectral Radiance at the sensor's aperture	$L\lambda = [0.0003342 * \text{Band}10) + 0.1]$	meter squared * ster * μm
		Centre wavelength of emitted radiance	$\lambda = 10.9$	μm
		Planck's constant	$h = 6.626 \times 10^{-34}$	Joules.secs
		The constant $\rho = h * c / \sigma$	$\rho = (\text{results} * 1 \times 10^6 \text{ to convert to micrometer from metre})$	micrometre.Kelvin
Land Surface Temperature in Kelvin	$T = TB / [1 + (\lambda * TB / \rho) \ln \varepsilon]$	Boltzmann constant	$\sigma = 1.38 \times 10^{-23}$	Joules/Kelvin
		Velocity of light	$C = 2.998 \times 10^8$	Metres/secs
		NDVI	$\text{NIR}(\text{Band}5) - \text{Red}(\text{Band}4) / \text{NIR}(\text{Band}5) + \text{Red}(\text{Band}4)$	-1 to 1 (unit less)
		Proportion of vegetation	$\text{PV} = (\text{NDVI}_f - \text{NDVI}_s) / (\text{NDVI}_f + \text{NDVI}_s)$ f=NDVI full cover, s=NDVI for bare soil	-1 to 1 (unit less)
		Land Surface Emissivity	$\varepsilon = (0.00149 * \text{PV}) + 0.98481$	Unitless
Conversion from Kelvin to Celsius	$T^\circ = T - 273.15$	LST in Kelvin	T	Kelvin
		LST in Celsius	T ^o	Celsius

depth of 0.6m and maximum at 22.5m. The deepest point just after construction was 27m as given by Bauchi State Sewerage and Water Corporation. This indicates sediment deposits over the fourty-year period of the dam. The shallowest areas have depth of 0.6m greater than the manual tide gauge reading ranging from 0.4m to 1.56m taken during the survey. However, these areas are less than the incoming streams to the dam with depth of 0.9m.

Table 3: Capacity and volume of Gubi Dam

Capacity		87, 847, 976.34m ³
Volume	Trapezoidal Rule	87, 848, 092.41m ³
	Simpson's Rule	87, 924, 252.35m ³
	Simpson's 3/8 Rule	87, 807, 274.28m ³

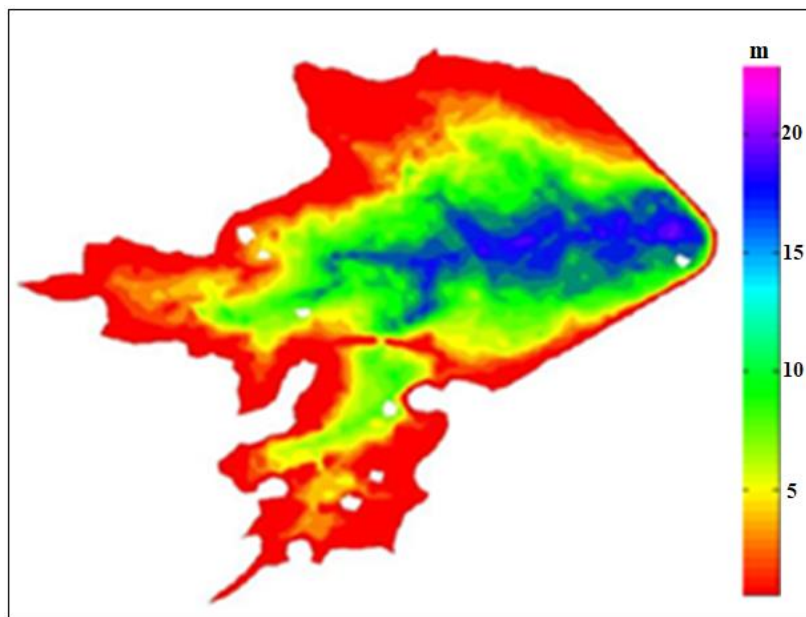


Figure 2: Two-dimensional bathymetric chart model showing minimum depth of 0.6m and maximum at 22.5m.

Water surface area and coverage

The condition of water surface for Gubi Dam is mapped for March of each year using normalized difference water index (NDWI) based on McFeeters (1996). From March 2017 to March 2020, there is a drastic change in water level which reflects low volume content (figure 3). This occurs likely due to excessive use of the water by inhabitants of Bauchi. Two scenarios could explain this: 1) improvement in water supply facilities in Bauchi metropolis making ease to consumption, 2) impact of recent federal policy on agriculture in 2015, where by a large number of Nigerians engage in farming practices due to border closure on importation of food items and high incentives coming from the government. This require drawing much water from the dam for irrigation purpose. We have not found a condition relating this water usage to rural-urban migration to Bauchi. However, communities located around riverine areas recharging Gubi may also be involved in irrigation and affecting the recharge. The year 2020 shows a smoother polygon, attributable to small change across the edges due to cloud affecting the thermal band and reducing areas in shallow areas. This shows that even though cloud cover is less than 2%, measurements can still be affected while using indices involving the thermal band.

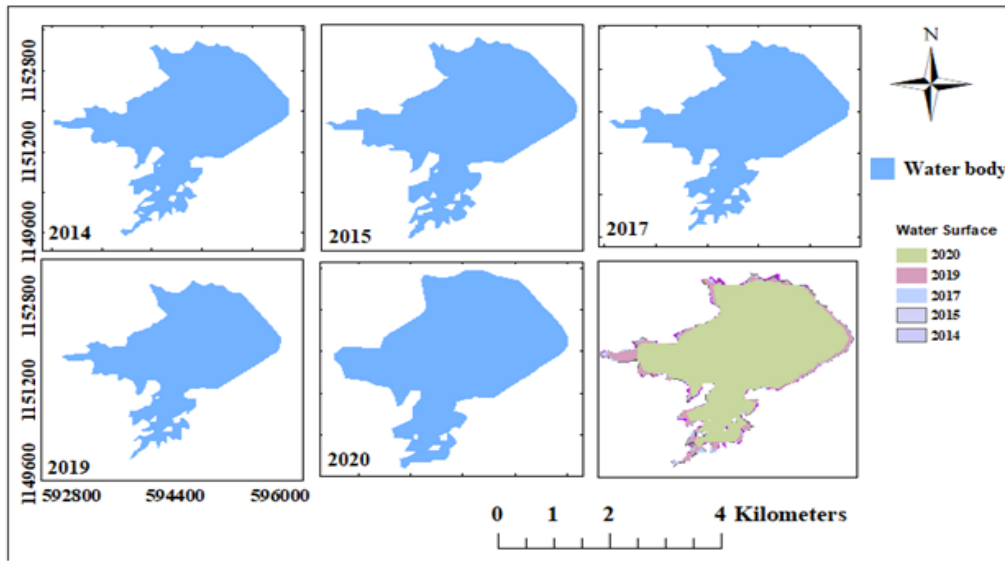


Figure 3: The water surface area coverage of each year. The external polygons were determined using normalised difference water index – NDWI. Note 2020 has the lowest water level in the vector overlay.

Peaks in the total area in hectares for each year as compared with the deviations from the mean is shown in figure 4. The years 2014 and 2015 were above average, while 2017 is just a little less than average. However, 2020 shows significant anomaly with values before the mean, reaching nearly 50 hectares. While the spatial distribution of land surface water reflects the storage and usage status of water resources on land surface (Foley *et al.*, 2005), its fluctuation might be related to climatic change (Oki and Kanae, 2006) when population dynamics is put into consideration. However, if it were possible to measure rural-urban migration into Bauchi metropolis, increase in population would have explained this scenario. To clear the enigma, we suggest that improvement in local agricultural productively due to improved incentives from government and border closure to food items lead to massive irrigation leading to reduction in water volume. Previous studies have shown that population growth and irrigation activities put much pressure on the dams (Bhattacharjee and Nayak, 2019; Enqvist and Ziervogel, 2019).

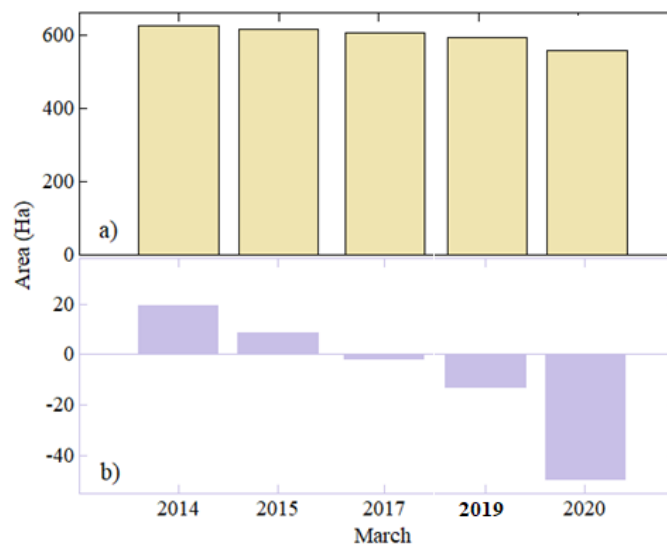


Figure 4: Surface area in hectares of Gubi Dam for five years, a) absolute values per year, b) deviations from the of 5-year absolute values.

Land Surface Temperature

The dam area and its surroundings are mapped to show land surface temperature (figure 5). These maps show variation in temperature of the dam and the areas around it. The coldest area is at the centre of the dam with values around 32°C, while warmest is on land that is nearly 45°C. The surface area of the water changes each year as evidently shown by the cropping up bathymetry with moderate temperatures and low water level in some years.

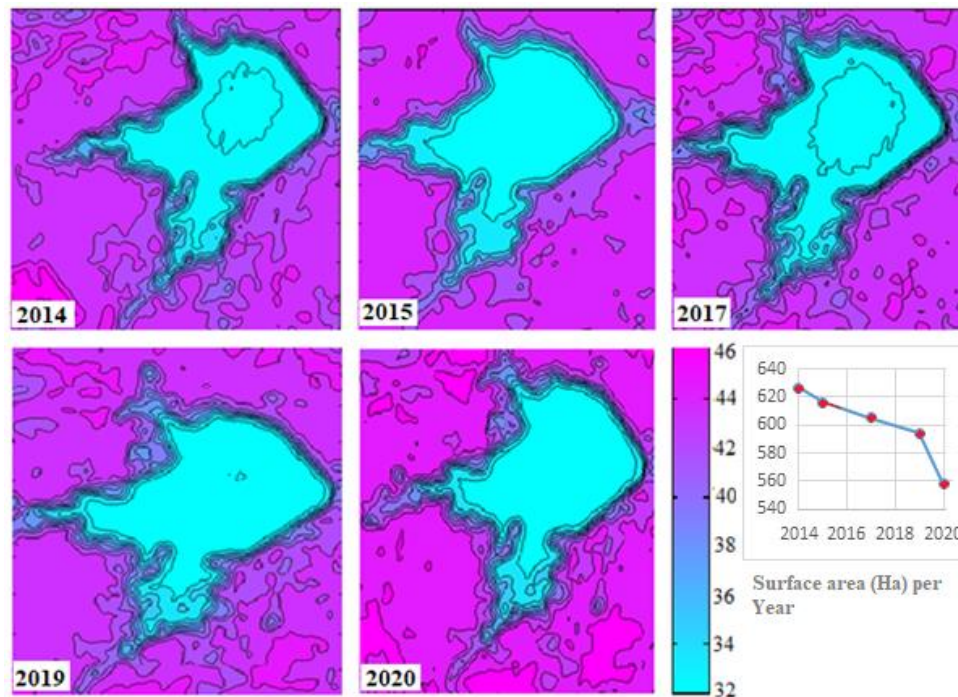


Figure 5: Contours of LST covering the lake (coldest) and its surrounding area (warmest). There is a steady decline in water from 2014 to 2020 as shown in the surface area per year to the right. Note the years considered are indicated by red dots.

Comparison of Surface area and surface temperature

The surface area of the dam over the March period of each year is further compared with temperature covering the whole area with the lake inclusive. This is to observe possible linkages between water content and temperature, for the fact that evaporation can play a significant role in maintaining water content. Hence LST has direct influence on evaporation. The years 2014, 2017 and 2019 gave a similar pattern while 2015 and 2020 gave a different connection between surface area and temperature as indicated by the bar peaks (figure 6).

Because the values of surface area in hectares and temperature in Celsius are different, we computed in percentage of total for each variable (figure 6). The relationships gave correlation (not shown) with $R^2 = 0.37$. This correlation is due to the observed variation between temperature and water level years 2014/2017/2019 compared to 2015/2020.

Although, land surface temperature provides a background information in and around the dam as previously studied by Valor and Caselles (1996) and Cheng *et al.* (2010), this instantaneous observations has secondary input to the overall studies of water volume of a reservoir. Other related geophysical information of land surface such as net evapotranspiration is required to give an overall view of the changes occurring.

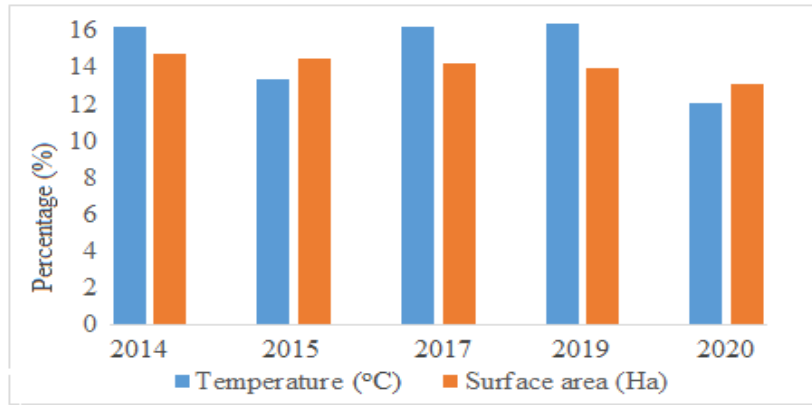


Figure 6: Percentage Land Surface Temperature (water and land) in comparison with water surface area.

Evaporation from impounded reservoirs may reduce the yield from a catchment areas by a considerable amount. This amount lost depend upon temperature of the air and water, wind, velocity, and atmospheric humidity. Figure 7a shows the mean rainfall pattern for Bauchi metropolis, close to Gubi Dam. Highest rainfall is observed in August followed by July. These marked the period of high humidity (figure 7b) and full recharge of the dam with water flowing from the adjoining rivers. This indicates that the dam’s capacity can only be fully reached when it is August.

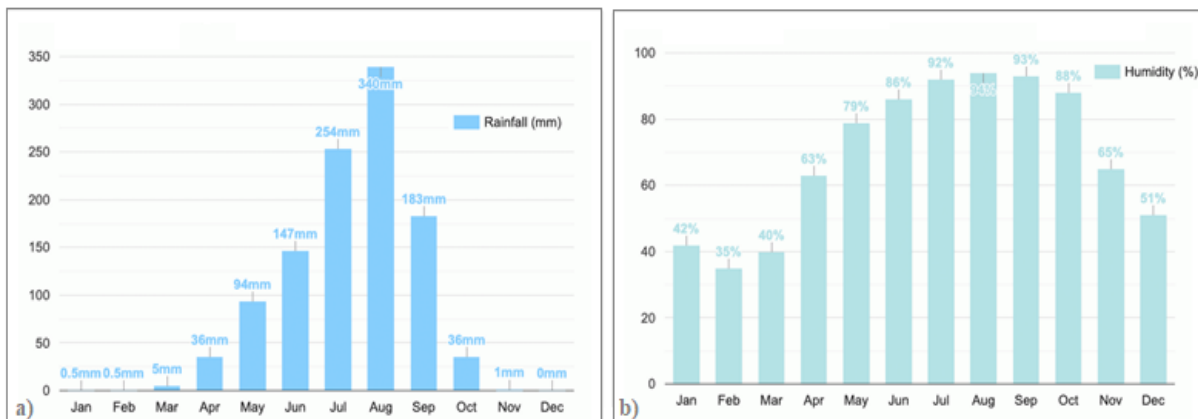


Figure 7: Climatic parameters of Bauchi, a) Mean annual rainfall (mm), and b) Mean annual relative humidity (%). Note the peaks in rainfall in August replicating the peak in relative humidity in August.

CONCLUSION

Observations and modeling of terrestrial water cycle is important for sustainable management of water resources as well as understanding the impact of climate change. Observational instruments focusing on spatio-temporal variability is important, and in this case multiplatform and multisensor instruments. The acoustic bathymetric technique using side scan sonar provides information at depth necessary for area and volume calculations while satellite provides area changes and quality of water. The single beam sonar used in this study helped calculate the water volume using three techniques that gave similar results. The water surface area shows the changing water surface signifying changes in volume. Together these techniques provide a unique way of mapping the dam bed as well as time-variability analysis

of volume. White satellite techniques are easy, in situ based sampling are expensive and laborious. However, bathymetric sampling at least once a year choosing during a favourable month would together with satellite data provide a broad study of the dam including sediment budget. This dam is already overdue in terms of dredging off sediments as the capacity during construction is not attainable currently due to sediments. This is necessary if the population growth of Bauchi metropolis and irrigated farming are put into consideration. In addition, water level measurement on Rivers Gubi, Ran, Tagwaye and Kura should be maintained to help monitor water level and compute discharge. Consistent gauge rainfall data should be available to study run off and recharge to the dam.

Globally, there is an increasing concern about the socio-economic and environmental costs of large dam. The theories and concepts of sustainability paradigm and their anticipated links to global environment change, economic and social crises must be linked to fresh water resource reservoirs such as Gubi Dam. Scenario-based analysis akin to strategic planning exercises and sustainability- related policies, rules, and regulations to the core thrust of environmental sustainability emerging strategies should be developed. These can be assessed based on SWOT analysis, linking strengths by opportunities and weakness to threats.

Acknowledgement

The authors wish to thank the Bauchi State Water and Sewerage Cooperation for allowing them to participate in the job and for providing us with the for research purpose. The authors would also like to acknowledge there viewers for their valuable comments, which helped to improve this manuscript.

References

- Azua, S., Nnah, S. I. and Ikwueze, H. U. (2020). Spatio-temporal Variability of Landuse Landcover and its Impact on Land Surface Temperature in Zaria Metropolis, Nigeria. *FUTY Journal of the Environment*. Vol 14(1), 1-11.
- BASWB/TP/037 (1990). Bauchi State water Board Technical Paper. Documentary of Gubi dam water supply scheme, Ramadan Printing Press , Bauchi, P4.
- Bhattacharjee, S., & Nayak, P. K. (2019). PV-pumped energy storage option for convalescing performance of hydroelectric station under declining precipitation trend. *Renewable Energy*, 135, 288-302.
- Boretti, A., & Rosa, L. (2019). Reassessing the Projections of the World water Development Report. *NPJ Clean Water*, 2(1), 1-6.
- Cheng, J.; Liang, S.; Wang, J.; Li, X. (2010). A stepwise Refining Algorithm of Temperature and Emissivity Separation for Hyperspectral Thermal Infrared data. *IEEE Trans. Geosci. Remote Sens.* 48, 1588–1597.
- Cheng, J., Liu, Q., Li, X., Qing, X., Liu, Q. and Du, Y. (2008). Correlation-based temperature and emissivity separation algorithm. *Sci. China Ser. D Earth Sci.*, 51,363–372.
- Connor, R. (2015). *The United Nations world water Development Report 2015: Water for a Sustainable World* (Vol. 1). Place de Fontenoy: UNESCO publishing.
- Elvenes, S., Buhl-Mortensen, P., and Dolan, M. F. J. (2012). Evaluation of alternative bathymetry data sources for MAREANO: a comparison of Olex bathymetry and multibeam data for substrate and biotope mapping. NGU Report 2012.030. Geological Survey of Norway, Trondheim, Norway. 54 pp
- Enqvist, J. P., & Ziervogel, G. (2019). Water Governance and Justice in Cape Town: An overview. *Wiley Interdisciplinary Reviews: Water*, 6(4), e1354.
- Foley, J. A. Gregory, R. D. and Barford, C. (2005). Global consequences of land use. *Science*, 309-570. doi:10.1126/science.1111772.

- Gao, B. C., (1996). NDWI—a normalized difference water index for remote sensing of vegetation liquid water from space. *Remote Sensing of Environment*, 58, pp. 257–266.
- Ghaleb, F., Mario, M. and Sandra, A. N. (2015) Regional Landsat-Based Drought Monitoring from 1982 to 2014. *Climate (MDPI)*. Vol 3, 563-577; doi:10.3390/cli3030563
- Haris, K., Chakraborty, B., Ingole, B., Menezes, A., and Srivastava, R. (2012). Seabed habitat mapping employing single and multi-beambackscatter data: a case study from the western continental shelf of India. *Continental Shelf Research*, 48: 40–49.
- Khatri, N., & Tyagi, S. (2015). Influences of natural and anthropogenic factors on surface and groundwater quality in rural and urban areas. *Frontiers in Life Science*, 8(1), 23-39.
- Larsen, T. A., Hoffmann, S., Lüthi, C., Truffer, B., & Maurer, M. (2016). Emerging solutions to the water challenges of an urbanizing world. *Science*, 352(6288), 928-933.
- Li, W. Du, Z. Ling, F. Zhou, D. Wang, H. Gui, Y. Sun, B. Zhan, X.A. (2013). A comparison of land water surface mapping using normalized difference water index from TM, ETM+ and ALI. *Remote sensing*, 5530-5549.
- Loucks, D. P., & Van Beek, E. (2017). *Water resource Systems Planning and Management: An Introduction to Methods, Models, and Applications*. Berlin: Springer.
- Manzo-Delgado, L., Sánchez-Colón, S. and Álvarez, R. (2009). Assessment of Seasonal Forest fire risk using NOAA-AVHRR: A case study in central Mexico. *Int. J. Remote Sens.* Vol 30, 4991–5013.
- McFeeters, S.K. (1996). The use of the normalized difference water index (NDWI) in the delineation of open water features. *Int. J. Remote Sens.* 17(1425–1432).
- Moradi, M; Sahebi, M; Shokri, M. (2017). Modified optimization water index (MOWI) for landsat 8 OLI/TIRS, . The international archives of the photogrammetry, remote sensing and spatial information sciences. Tehran’s joint ISPRS conference of GI research, SMPR and EOEC, 7-10 Oct.
- Oki, T. Kanae, S. (2006). Global hydrological cycles and world water resources. *Science*, 313:1068. doi:10.1126/science.1128845.
- Page, D., Bekele, E., Vanderzalm, J., & Sidhu, J. (2018). Managed aquifer recharge (MAR) in sustainable urban water management. *Water*, 10(3), 239.
- Papa, F., Prigent, C. and Rossow, W. B. (2008). Monitoring flood and discharge variations in the large Siberian Rivers from a multi-satellite technique. *Surv. Geophys.* Vol 29, 297–317.
- Parnum, I., Siwabessy, J., Gavrillov, A., and Parsons, M. (2009). A Comparison of Single Beam and Multibeam Sonar Systems in Sea floor Habitat Mapping. Underwater Acoustic Measurements: Technologies & Results, 3rd International Conference and Exhibition, Napoleon, Greece.
- Roberts, N.; Taieb, M.; Barker, P.; Damnati, B.; Icole, M.; Williamson, D. (1993). Timing of the younger dry as event in east-Africa from lake-level changes. *Nature*, 366, 146–148.
- Schimel, A. C. G., Healy, T. R., Johnson, D., and Immenga, D. (2010a). Quantitative experimental comparison of single-beam, sidescan, and multibeam benthic habitat maps. *ICES Journal of Marine Science*, 67: 1766–1779.
- Schimel, A. C. G., Healy, T. R., McComb, P., and Immenga, D. (2010b). Comparison of a Self-Processed EM3000 Multibeam Echo sounder Dataset with a QTC View Habitat Mapping and a Sidescan Sonar Imagery, Tamaki Strait, New Zealand. *Journal of Coastal Research*, 26: 714–725.
- Serpetti, N., Heath, M., Armstrong, E., and Witte, U. (2011). Blending single beam RoxAnn and multi-beam swathe QTC hydro-acoustic discrimination techniques for the Stonehaven area, Scotland, UK. *Journal of Sea Research*, 65: 442–455.
- Sims, D. A., & Gamon, J. A. (2003). Estimation of vegetation water content ndphotosynthetic

- tissue area from spectral reflectance: a comparison of indices based on liquid water and chlorophyll absorption features. *Remote Sensing of Environment*, 84, 526–537.
- Singh, R. P. and Gupta, P. K. (2016). Development in remote sensing techniques for hydrological studies, *procindiannatnsiacad* vol. 82 no. 3, pp. 773-786.
- Sobrino, José A., Juan C. Jiménez-Muñoz, and Leonardo Paolini (2016). "Land Surface Temperature Retrieval from LANDSAT TM 5." *Remote Sensing of Environment* 90.4 (2004): 434-40. Web. Mar. 2016. <http://www.uv.es/ucg/articulos/2005/Publications_2004_10.pdf>
- Tang, Z; Qu, W; Dai, Y; Xin, Y. (2013). Extraction of water body based on lansat TM5 imagery: A case study in the Yangtze river. *Advanced information communication technology*, 416-420.
- Tendai, S. (2005). Estimation of small reservoir storage capacities in Limpopo river basin using geographical information systems (GIS) and remotely sensed surface areas. Master thesis. Department of Civil Engineering, University of Zimbabwe.
- Tukur, A.L., Mubi, A.M. Impact of Kiri dam on the lower reaches of River Gongola, Nigeria. *GeoJournal* 56, 93–96 (2002). <https://doi.org/10.1023/A:1022449113407>.
- Valor, E.; Caselles, V. (1996). Mapping land surface emissivity from ndvi: Application to european, African and south American areas. *Remote Sens. Environ.* Vol 57, 167–184.3.
- Vorosmarty, C. J., Sharma, K. P., Fekete, B. M., Copeland, A. H., Holden, J. Marble, J. and Lough, J. A. (1997). The storage and aging of continental runoff in large reservoir systems of the world. *AMBIO*, 26, 210–219.
- Wan, Z. and Dozier, J. (1996). A generalized split-window algorithm for retrieving land-surface temperature from space. *IEEE Trans. Geosci. Remote Sens.* Vol 34, 892–905.
- Weng, Q., Lu, D. and Schubring, J. (2004). Estimation of land surface temperature–vegetation abundance relationship for urban heat island studies. *Remote Sens. Environ.* Vol 89, 467–483.5.
- World Water Council (2018). *Global Water Security, Lessons Learnt and Long-Term Implications*. Springer Series. Preface I. pp vii-viii. <http://www.springer.com/series/7009>
- Wufem, B. M., Ibrahim, A. Q., Gin, N. S., Mohammed, M.A., Ekanem, E. O. and Shibdawa, M.A. (2009). Speciation of Heavy Metals in the Sediments of Gubi Dam, Bauchi State, Nigeria. *Global Journal of Environmental Sciences*. Vol. 8 (2), 55-63.
- Xu, H.Q. (2006) Modification of normalised difference water index (NDWI) to enhance open water features in remotely sensed imagery. *Int. J. Remote Sens.* 27 (3025–3033).
- Zhou, H; Hong, J; Huang, O. (2011). Landscape and water quality change detection in urban wetland. A post classification comparison method with IKONOS data procedia. *Environmental sciences*, 1726-1731.



© 2020 by the authors. License FUTY Journal of the Environment, Yola, Nigeria. This article is an open access distributed under the terms and conditions of the Creative Commons Attribution (CC BY) license (<http://creativecommons.org/licenses/by/4.0/>).